Surface instability and isotopic impurities in quantum solids

E. Cappelluti,[1,2] G. Rastelli,[2,3] S. Gaudio,[2] and L. Pietronero[1,2]
[1]*SMC Research Center and ISC, INFM-CNR, Via dei Taurini 19, 00185 Rome, Italy*
[2]*Dipartimento di Fisica, Università "La Sapienza," Piazzale Aldo Moro 2, 00185 Rome, Italy*
[3]*Laboratoire de Physique et Modélisation des Milieux Condensés, Université Joseph Fourier, CNRS-UMR 5493, Boite Postale 166, 38042 Grenoble, France*
(Received 13 November 2007; revised manuscript received 11 January 2008; published 7 February 2008)

In this paper, we employ a self-consistent harmonic approximation to investigate surface melting and local melting close to quantum impurities in quantum solids. We show that surface melting can occur at temperatures much lower than the critical temperature T_c of the solid phase instability in the bulk. Similar effects are driven by the presence of an isotope substitution. In this latter case, we show that stronger local lattice fluctuations, induced by a lighter isotope atom, can induce local melting of the host bulk phase. Experimental consequences and the possible relevance in solid helium are discussed.

DOI: 10.1103/PhysRevB.77.054301 PACS number(s): 63.20.Ry, 67.80.−s, 68.08.Bc

I. INTRODUCTION

Although melting is a very common phenomenon in nature, the debate about its microscopic mechanism is still open.[1–3] The first empirical theory was advanced by Lindemann.[4] According to this view, melting occurs when the ratio between the root mean square (rms) $u_{\mathrm{rms}}=\sqrt{\langle u^2\rangle}$ of the thermally activated lattice fluctuations and the lattice constant a exceeds a phenomenological threshold $u_{\mathrm{rms}}/a \gtrsim 0.16$ which is roughly material independent.[5,6] In spite of its several flaws (melting is described in terms of the properties of only the solid phase; no cooperative process and no role of defects are considered), this simple criterion seems to work reasonably well for a variety of materials.[7] The Lindemann criterion has been recently found to apply as well at a *local* level around crystal defects.[8,9] This large range of validity of the Lindemann criterion suggests thus that a microscopic mechanism is actually operative.

The most simple (and employed) model to account for the Lindemann phenomenology is the self-consistent harmonic approximation (SCHA). This maps an anharmonic phonon model in a harmonic one. Anharmonicity is, then, taken into account, at a mean-field level, through a Debye-Waller-like term which is evaluated self-consistently. The breakdown of this approach is interpreted as a signal of solid phase instability and hence related to melting. One of the strength of this theory is that it predicts, in contrast with the Born criterion but in agreement with the experimental observation, a partial but not total softening of the elastic constants of the bulk.

The SCHA represents, moreover, an efficient tool to understand in a qualitative way the phenomenon of the surface melting (SM), as first proposed by Pietronero and Tosatti (PT).[10] In this context, the physical mechanism underlying the surface melting is quite simple: atoms close to the surface have larger lattice fluctuations due to the reduced number of nearest neighbor sites, and the SCHA breaks down consequently at smaller temperatures than in the bulk. It is clear that this simple theory does not represent an exhaustive description of the surface melting phenomenology, which should include roughening, preroughening, partial wetting, the role of "crystallinity," etc.[11,12] In addition, it should be stressed that the SCHA does not determine directly the melting point but rather the instability of the solid phase which is prevented by the melting process itself.[13] In this perspective, this criterion should not be employed at a quantitative level. Nevertheless, since the solid phase instability and the actual melting process are usually related to each other, the PT theory provides a simple and useful way to get information about the tendency of a system toward melting and surface melting and their dependence on microscopic parameters.

In this paper, we generalize the results of the PT approach in the case of quantum solids. The Lindemann criterion in the quantum solid is shown to be twice as large as the one in the classical limit, in agreement with experimental reports.[14] We show a phase diagram for both the bulk and surface melting cases, and we investigate also the local melting due to an isotopic substitution. The temperature dependence of the lattice fluctuations for the different classical and/or quantum regimes is evaluated and also the profile of the lattice fluctuations as a function of the distance from the surface or the isotopic impurities. The paper is organized as follows. In Sec. II, we review the approach of Pietronero and Tosatti for classical solids. In Sec. III, we generalize the PT approach to investigate bulk properties in quantum solids, surface melting and solid phase instability close to a quantum isotope impurity are analyzed, respectively, in Secs. IV and V. Finally, in Sec. VI, we discuss our results and draw some final conclusions.

II. SELF-CONSISTENT HARMONIC APPROXIMATION AND SOLID PHASE INSTABILITY IN BULK AND ON SURFACES

Let us consider for simplicity a one-dimensional chain of atoms. At the harmonic level, we can write the equations of motion for the lattice displacement u_n,

$$M\ddot{u}_n + \frac{k_{n,n+1}}{2}(u_n - u_{n+1}) + \frac{k_{n,n-1}}{2}(u_n - u_{n-1}) = 0, \qquad (1)$$

where M is the atomic mass and n denotes the site index. The constant forces $k_{n,n'}$, at the harmonic level, are related to the

interatom potential $V_{n,n'}$ through the relation $k_{n,n'} = \partial^2 V_{n,n'}/\partial u_n^2|_{\{u_n\}=0}$. Writing the potential $V_{n,n'}$ in terms of a Fourier expansion, $V_{n,n'}=\Sigma_q V_q \exp[iq(u_n-u_{n'})]$, we have thus, at the harmonic level, $k_{n,n'}=k_0=-\Sigma_q q^2 V_q$.

In the spirit of SCHA, anharmonic terms can be taken into account, by replacing the constant forces $k_{n,n'}$, evaluated at the lattice equilibrium, with their expectation value $\tilde{k}_{n,n'}$ averaged over the lattice fluctuations. We have thus explicitly

$$\tilde{k}_{n,n'} = \left\langle \frac{\partial^2 V_{n,n'}}{\partial u_n^2} \right\rangle = -\sum_q q^2 V_q \exp[-q^2\langle |u_n - u_{n'}|^2\rangle/2] \simeq k_0 \exp[-\lambda\langle u_n^2\rangle/2 - \lambda\langle u_{n'}^2\rangle/2], \quad (2)$$

where in the last line, we have neglected the cross terms and we have replaced the dependence on the momenta in the exponential with an effective parameter λ.

By inserting Eq. (2) in Eq. (1) and considering the motion of each atom as an Einstein oscillator, we have

$$M\ddot{u}_n + \frac{1}{2}[\tilde{k}_{n,n+1} + \tilde{k}_{n,n-1}]u_n = 0, \quad (3)$$

where anharmonic effects are taken into account in the self-consistent renormalization of the elastic constants $\tilde{k}_{n,n'}$. Note that $\tilde{k}_{n,n'}$ depends on the expectation value of the quadratic lattice fluctuations on both sites n, n'. It follows that the atomic motion described in Eq. (3) is ruled by the lattice fluctuations of the lattice *environment*. In a bulk system, $\langle u_n^2\rangle = \langle u_{n'}^2\rangle = \langle u^2\rangle$, then

$$\tilde{k}_{n,n'} = \tilde{k} = k_0 \exp[-\lambda\langle u^2\rangle], \quad (4)$$

and we get a unique self-consistent equation,

$$\langle u^2\rangle = \frac{k_B T}{\tilde{k}} = \frac{k_B T}{k_0} \exp[\lambda\langle u^2\rangle], \quad (5)$$

where k_B is the Boltzmann constant. In similar way, the SCHA phonon frequency is given by $\tilde{\omega}_0 = \sqrt{\tilde{k}/M} = \omega_0 \exp[-\lambda\langle u^2\rangle/2]$, where $\omega_0 = \sqrt{k_0/M}$ is the bare phonon frequency at the purely harmonic level. It is convenient to rewrite Eq. (5) by introducing the dimensionless quantities $y=\lambda\langle u^2\rangle$, $\tau_{\rm cl}=\lambda k_B T/k_0$,

$$y(\tau_{\rm cl}) = \tau_{\rm cl} e^{y(\tau_{\rm cl})}. \quad (6)$$

Equation (6) has no solution for $\tau_{\rm cl} \geq \tau_{\rm cl}^{\rm max} = 1/e = 0.368$, which determines a critical temperature $k_B T_c = 0.368 k_0/\lambda$. At this value, $y(\tau_{\rm cl}^{\rm max})=1$ and the maximum magnitude of the allowed lattice fluctuations above which the solid phase is unstable is $\langle u^2\rangle^{\rm max} = 1/\lambda$. Note that $\langle u^2\rangle^{\rm max}$ depends neither on the atomic mass nor on the force constant k_0, in agreement with the observation of similar Lindemann ratios in materials with extremely different phonon frequencies and atomic masses.

Equation (3) represents also the starting point to apply the SCHA to surface melting. In this case, one defines a local average lattice fluctuation $\langle u_n^2\rangle$ which depends on the site index n. In the same spirit, one can define a local elastic constant,

$$\tilde{k}_{n,n-1,n+1} = [\tilde{k}_{n,n+1} + \tilde{k}_{n,n-1}] = k_0 e^{-\lambda\langle u_n^2\rangle/2}[e^{-\lambda\langle u_{n-1}^2\rangle/2} + e^{-\lambda\langle u_{n+1}^2\rangle/2}]. \quad (7)$$

We can write thus a set of recursive equations where the lattice fluctuations of the atom n depend on the lattice fluctuations of the $n-1$ and $n+1$ atoms. The recursion is truncated at the atom $n=1$ which represents the outer atom close to the free surface. This atom probes an effective harmonic potential smaller than the bulk, which increases its tendency toward melting. A numerical solution shows that the solid phase for the surface atoms becomes unstable at $\tau_{\rm cl}^{\rm SM}=0.271$, 26% smaller than the bulk value. The same theory permits the evaluation of the profile of the lattice fluctuations as a function of the distance from the surface. These theoretical predictions agree quite well with the profile of the lattice fluctuations close to defects (grain boundaries, dislocations, and vacancies) in colloidal solids.[9] Note that, although the temperature of surface melting is smaller than that in the bulk, local lattice fluctuations of the outer atoms can be *larger* than the ones in the bulk, violating locally the Lindemann criterion. This is also in agreement with Ref. 9. For instance, for the outer atoms $n=1$, one finds $y_1^{\rm SM}=1.74$. This is 74% larger than the value in the bulk.

III. BULK PROPERTIES OF QUANTUM SOLIDS

The melting process of quantum solids has been discussed in many papers, mainly by using approaches based on the density functional theory.[15–19] However, they are, in general, quite hard to be employed to investigate premelting effects close to local defects. To this aim, we generalize now the above presented PT theory, which presents the advantages to be easily generalized in a local framework, to the case of quantum solids. In the following, we shall assume a one-particle picture to be still valid because of the smallness of the exchange terms in the solid phase ($J^{\rm max}\sim 0.1$ K in ^{4}He, $J^{\rm max}\sim \mu$K in ^{3}He) with respect to the melting temperatures $T_m \gtrsim 2$ K.[20,21] On the other hand, a major role in our approach will be played by the quantum fluctuations which dominate at low temperature in the quantum regime. According to this perspective, the atomic motion of the atom n is described in terms of the SCHA Hamiltonian of the quantum oscillator,

$$\left[-\frac{\hbar^2\nabla_u^2}{2M} + \frac{1}{4}\tilde{k}_{n,n-1,n+1}u_n^2\right]\Psi(u_n) = E\Psi(u_n), \quad (8)$$

where the self-consistent expression for the local potential $\tilde{k}_{n,n-1,n+1}$ is reported in Eq. (7).

We consider first the melting properties of bulk systems ($\tilde{k}_{n,n-1,n+1}=2\tilde{k}$). In this SCHA quantum model, the total amount of lattice fluctuations is now easily computed as

$$\langle u^2\rangle = \frac{\hbar}{2M\tilde{\omega}_0}\left[1 + 2n\left(\frac{\hbar\tilde{\omega}_0}{k_BT}\right)\right], \tag{9}$$

where $n(x)=1/[e^x-1]$ is the Bose factor and where we remind $\tilde{\omega}_0=\sqrt{\tilde{k}/M}$ and $\tilde{k}$ is given by Eq. (4). In the classic limit, $k_BT \gg \hbar\tilde{\omega}_0$, $n(x)\simeq 1/x \gg 1$, and we recover the classical result of Eq. (5). On the other hand, in the zero temperature limit, lattice fluctuations are due only to zero point quantum motion. In this case, $n(x)=0$ and Eq. (9) reads

$$\langle u^2\rangle = \frac{\hbar}{2\sqrt{M\tilde{k}}} = \frac{\hbar}{2\sqrt{Mk_0}}\exp[\lambda\langle u^2\rangle/2], \tag{10}$$

which, introducing the variable $\tau_Q=\lambda\hbar/2\sqrt{k_0M}$, can be written in the dimensionless form

$$y(\tau_Q) = \tau_Q e^{y(\tau_Q)/2}. \tag{11}$$

Equation (11) represents the quantum generalization of Eq. (6) where the instability of the solid phase is now triggered by the magnitude of the quantum lattice fluctuations. This occurs for $\tau_Q \geq \tau_Q^{\max}=2/e=0.736$. It is interesting to note that the breakdown of the solid phase driven by quantum fluctuations is not merely equivalent to the one related to the thermal motion. Indeed, for a quantum solid, we would predict a maximum magnitude of lattice fluctuations $y(\tau_Q^{\max})=2$, *two times* larger than for classical solids. This behavior is indeed in agreement with the report of the Lindemann ratio $u_{\rm rms}/a\simeq 0.28$ in helium solids[14,22,23] to compare with $u_{\rm rms}/a\simeq 0.16$ for classical solids.

We also consider now the general case where both thermal and quantum fluctuations are important. From Eq. (9), after few straightforward passages, we get

$$y(\tau_Q,\tau_{\rm cl}) = \tau_Q e^{y(\tau_Q,\tau_{\rm cl})/2}\left[1 + 2n\left(\frac{2\tau_Q}{\tau_{\rm cl}}e^{-y(\tau_Q,\tau_{\rm cl})/2}\right)\right]. \tag{12}$$

Equation (12) generalizes the stability criterion based on the SCHA in the full quantum-thermal case. As a general rule, we can expect that the classical regime is relevant in the empirical range $k_BT/\hbar\omega_0 \gtrsim 1/4$, which corresponds to $\tau_Q \lesssim 2\tau_{\rm cl}$, while in the opposite regime, $\tau_Q \gtrsim 2\tau_{\rm cl}$ quantum effects are dominant.

In Fig. 1, we show the phase diagram in the full τ_Q-$\tau_{\rm cl}$ space where the instability of the SCHA occurs. Along the boundary line, the critical lattice fluctuations increase smoothly from $y=1$ in the $\tau_Q=0$ case to $y=2$ in the $\tau_{\rm cl}=0$ case. Also interesting is the dependence of the lattice fluctuations as a function of $\tau_{\rm cl}$, namely, the temperature (Fig. 1, bottom panel). In the classical case, $\tau_Q=0$, the quadratic fluctuations $y\propto\langle u^2\rangle$ increase linearly with $\tau_{\rm cl}$ until anharmonic effects take place. Anharmonicity is reflected in a upturn of the temperature dependence of $y(\tau_{\rm cl})$ and eventually in the breakdown of the solid phase for $\tau_{\rm cl}=1/e$ and $y=1$. Increasing τ_Q leads not only to the presence of zero point motion quantum fluctuations at $\tau_{\rm cl}=0$ but also to an overall change of the temperature dependence of y. In particular, the range of the linear temperature dependence, characteristic of classical harmonic solids, is rapidly reduced and for strongly quantum solids, it disappears. Lattice fluctuations are large

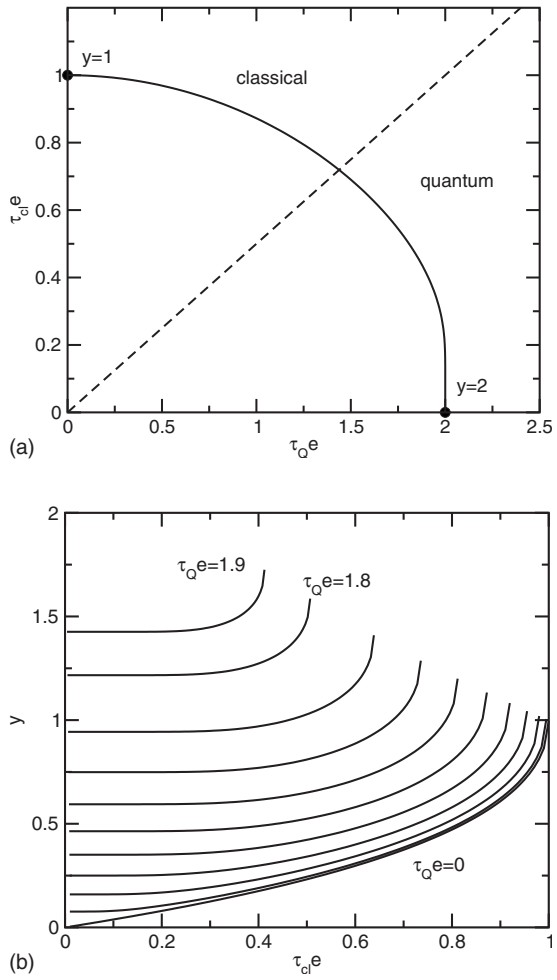

FIG. 1. (Top panel) Phase boundary of the SCHA in the τ_Q-$\tau_{\rm cl}$ space; (bottom panel) lattice fluctuations $y=\lambda\langle u^2\rangle$ as a function of the classical parameter $\tau_{\rm cl}$ for (from the bottom to the top) $\tau_Qe=0.2,0.4,0.6,\ldots,1.6,1.8,1.9$ (we remind that $\tau_Q^{\max}=2/e$).

already at $T=0$, and they are almost constants in a wide temperature range (note that in this regime, anharmonic effects are in any case present due to quantum fluctuations) until an abrupt upturn with the temperature leads to the breakdown of the solid phase. This trend is in good qualitative agreement with recent experimental measurements[24] and quantum Monte Carlo calculations.[25] We shall discuss them in detail in Sec. VI.

IV. SURFACE MELTING OF QUANTUM SOLIDS

After having investigated the bulk properties of quantum solids, we now analyze the role of quantum fluctuations on the surface melting. We can write a recursive set of equations by considering the quantum and/or thermal SCHA solution of the nth atom,

$$\langle u_n^2\rangle = \frac{\hbar}{2M\tilde{\omega}_n}\left[1 + 2n\left(\frac{\hbar\tilde{\omega}_n}{k_BT}\right)\right], \tag{13}$$

where $\tilde{\omega}_n=\sqrt{\tilde{k}_{n,n-1,n+1}/2M}$ and where the local elastic constant $\tilde{k}_{n,n-1,n+1}$ is still given by Eq. (7). Employing the usual

dimensionless variables τ_Q, τ_{cl}, y_n, we can thus write

$$y_n = \frac{\sqrt{2}\tau_Q e^{y_n/4}}{\sqrt{e^{-y_{n-1}/2} + e^{-y_{n+1}/2}}}\left[1 + 2n\left(\frac{2\tau_Q}{\tau_{cl}}\frac{\sqrt{e^{-y_{n-1}/2} + e^{-y_{n+1}/2}}}{\sqrt{2}e^{y_n/4}}\right)\right], \tag{14}$$

which is valid for any $n \geqslant 2$, while the outer atom $n=1$ obeys the relation

$$y_1 = \sqrt{2}\tau_Q e^{(y_1+y_2)/4}\left[1 + 2n\left(\frac{2\tau_Q}{\sqrt{2}\tau_{cl}}e^{-(y_1+y_2)/4}\right)\right]. \tag{15}$$

In order to obtain a numerical solution of Eqs. (14) and (15) for given τ_Q, τ_{cl} in the stable solid phase, we start by choosing a trial value of y_1. The full set of $\{y_n\}$ is thus obtained by Eqs. (14) and (15). The initial trial value of y_1 is thus varied until $y_{n=\infty}$ converges to its bulk value. Typically, this is the only physical solution, since $y_{n=\infty}$ diverges for larger values of y_1 while it becomes rapidly negative for smaller values of y_1. For τ_Q, τ_{cl} larger than some critical value, the procedure does not converge for *any* value of y_1, signalizing that the solid phase of the surface atom, described by the SCHA, is unstable.

The resulting phase diagram, in the full τ_Q-τ_{cl} space, is shown in Fig. 2 (top panel), where we compare the boundary of the surface melting instability (dashed line) with the one of the bulk melting (solid line). For the pure quantum case, $\tau_{cl}=0$, at zero temperature, the surface instability occurs for $\tau_Q^{SM}=0.664$ where the lattice fluctuations of the outer atoms become as large as $y_{1,Q}^{SM}=3.21$. It is interesting to note that, for $0.664 < \tau_Q < 0.736$, the surface is unstable *even* at zero temperature whereas the bulk solid phase is always stable up to a finite temperature range. The ratio T_c^{SM}/T_c between the surface melting temperature and the temperature of bulk melting is shown in the bottom panel of Fig. 2 showing that the critical temperature of surface melting can be significantly lower than the bulk one in quantum solids.

Before concluding this section, we would like to briefly compare the melting occurring at a free surface with other cases such as grain boundaries. In the case of a free surface, in going from Eq. (14) to Eq. (15), we have dropped in Eq. (15) the contribution of the $n=0$ atom. We note that the same results would be obtained in Eq. (14) considering $n=1$ and assuming the lattice fluctuations at the site $n=0$ to be infinite, namely, $y_{n=0}=\infty$. This latter condition would be obtained by the harmonic oscillator solution of Eq. (13) at the site $n=0$ with a vanishing elastic constant $\tilde{k}_{n,n-1,n+1}$, and it express nothing more than the condition that atoms for $n<1$ are not in a solid arrangement but in a gaseous phase.

An intermediate situation is encountered when melting at grain-boundary interfaces is considered. In this case, the outer atom $n=1$ of a grain would not probe a free surface at the site $n=0$, but it will interact with a lattice environment with a different arrangement. These two situations can be described by a similar set of recursion relations [Eq. (14)] but with different boundary conditions: in the free surface case, boundary conditions at site $n=0$ will be described by a completely soft oscillator $\tilde{k}_{n,n-1,n+1}=0$, signalizing that bulk solid is interfaced with a free gaseous phase; on the other hand, in the case of grain boundaries, the outer atom $n=1$ will still probe a crystal structure for $n \leq 0$, although with a different arrangement. The boundary conditions at site $n=0$ will still be described thus by Eq. (13), but with a not completely soft mode. We expect thus that melting processes occur as well at grain boundaries as in the case of free surface. From the mathematical point of view, this situation is identical to the case of quantum isotopic substitutions, and it will be discussed in detail in the next section.

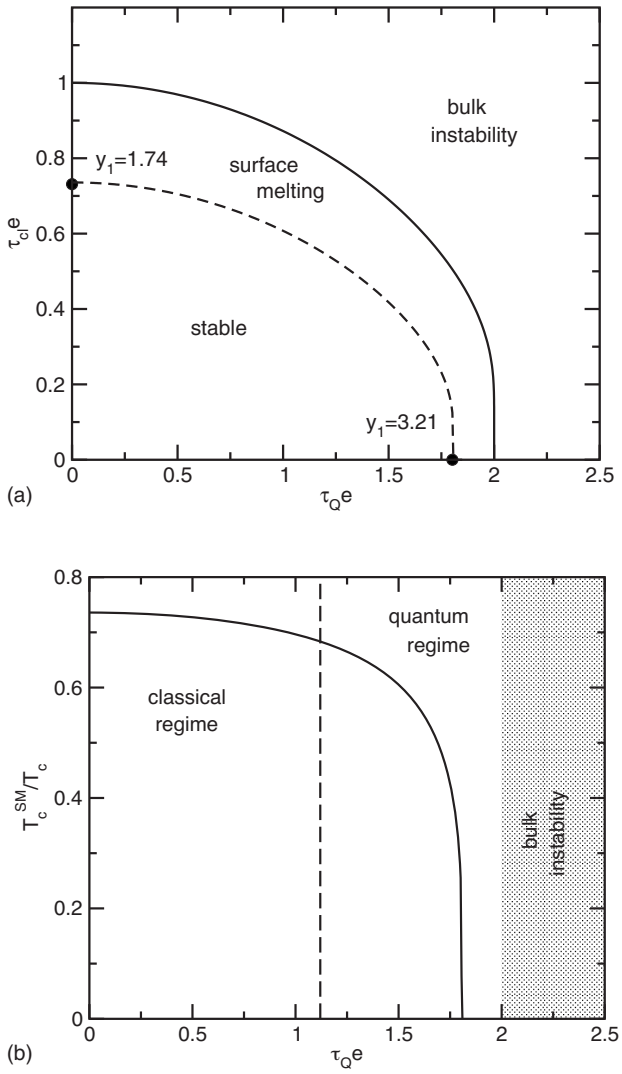

FIG. 2. (Top panel) Phase boundary for the surface melting instability (dashed line) compared with the bulk instability (solid line) in the τ_Q-τ_{cl} space; (bottom panel) ratio between surface melting temperature T_c^{SM} and bulk melting temperature T_c as a function of τ_Q. For $\tau_Q e$, even the bulk phase is unstable. For $1.12 < \tau_Q e < 2$, the system is in a quantum regime where $k_B T_c^{SM}/\hbar\tilde{\omega}_0 \lesssim 1/4$.

V. QUANTUM MELTING DRIVEN BY ISOTOPIC IMPURITIES

In this section, we address the problem of the solid phase stability close to a single local isotopic substitution embed-

ded in a perfect lattice structure. In the SCHA approach, local stability of the solid phase is given by the solution of Eq. (13). It is easy to check that, in the classical limit $k_BT \gg \hbar\tilde{\omega}_n$, the dependence on the atomic mass M in Eq. (13) drops out, so that different isotope solids should probe the same stability conditions. On the other hand, the mere observation of a different melting line for ^{4}He and ^{3}He is a direct evidence that helium is in a quantum regime.[26,27] Different isotopes are thus expected to affect the bulk solid phase stability. We expect the same at the local level.

In the following, we shall consider the case of an isolate substitution with a lighter isotope in a host matrix of heavier atoms. Quantum fluctuations in the two cases will be ruled locally by the parameters $\tau_L = \lambda\hbar/2\sqrt{k_0 M_L}$ and $\tau_H = \lambda\hbar/2\sqrt{k_0 M_H}$, respectively, for the lighter (L) and for the heavier (H) atoms. To study the stability of the solid phase close to this isotopic quantum impurity, we can still employ the recursive relations [Eq. (14)], namely, for $n \leq -1$, $n \geq 1$, we set $\tau_Q = \tau_H$, whereas for $n=0$ (quantum isotope impurity), we have $\tau_Q = \tau_L$. We shall consider the representative case of a ^{3}He impurity embedded in ^{4}He solid. In this case, $\tau_L/\tau_H = \sqrt{4/3}$. Same changes are, in principle, needed in this model in the case of local isotope impurities. While a one-dimensional geometry could be, indeed, appropriate to investigate melting effects close to flat surfaces, where only the linear distance from the surface matters, a true three-dimensional treatment is expected to be required when an isolate isotope impurity is embedded in a bulk matrix. For the sake of simplicity, however, we still employ the effective one-dimensional model described by Eq. (14). In this case, the atom index n should be meant as a Manhattan distance from the impurity. A careful treatment of dimensionality would of course affect the profile of the lattice fluctuations along different Manhattan lines and also affect the precise determination of the critical values for the solid phase instability. We notice, however, that the solid phase instability is mainly ruled by the first atomic layer in direct contact with the surface or with the isotope impurity and that the profile of the lattice fluctuations decays to their bulk value quite rapidly within a few lattice constants.[10] Along this perspective, we expect that a full inclusion of the dimensional effects would not change qualitatively our results.

In Fig. 3 (top panel), we show the phase diagram of the lattice instability of the host ^{4}He solid close to the quantum isotopic ^{3}He impurity. It is instructive to compare the classical limit $\tau_Q = 0$ with the pure quantum one $\tau_{cl} = 0$. In the first case, lattice fluctuations of the guest atom, as well as of the host atoms, are independent of the relative atomic mass and they depend only on the temperature. As a consequence, the solid phase close to the guest atom is completely unaffected by the isotopic substitution. A quite different situation occurs in the highly quantum regime $\tau_{cl} = 0$. In this case, local quantum lattice fluctuations of the lighter guest atom can be significantly enhanced due to its reduced atomic mass, and they can be sufficiently large to induce a local melting of the *host* solid phase. At $\tau_{cl} = 0$, this occurs for $\tau_H > 0.681$, not much higher than in the case of a free surface truncation ($\tau_Q > 0.664$). Note that Fig. 3 defines a region (quantum impurity melting) where the solid phase is still stable in the bulk but local quantum lattice fluctuations break down the solid

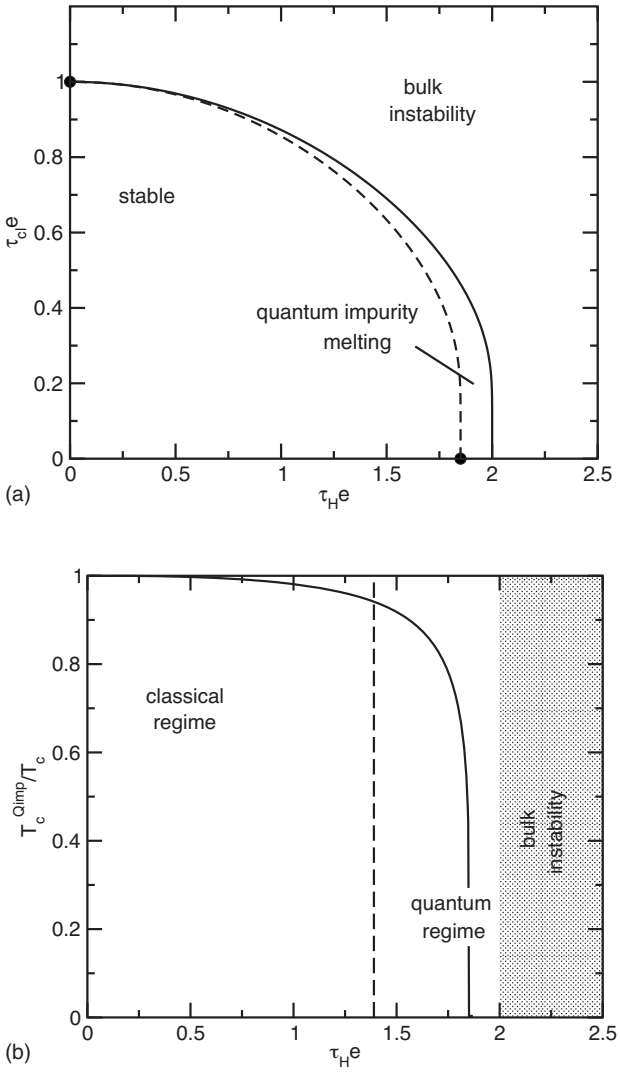

FIG. 3. (Top panel) Phase boundary for the lattice instability around a quantum isotopic substitution with $\tau_L/\tau_H = \sqrt{4/3}$ (dashed line) compared with the bulk instability (solid line); (bottom panel) ratio between melting lattice temperature T_c^{Qimp} around the quantum impurity and bulk melting temperature T_c as a function of host quantum parameter τ_H. In the quantum regime, $1.39 < \tau_H e < 2$, where $k_B T_c^{Qimp}/\hbar\tilde{\omega}_0 \leq 1/4$, the local melting temperature around the quantum impurity is sensibly lower than that in the bulk, and for $1.85 < \tau_H e < 2$, solid phase around isotopic quantum impurities is unstable even at $T=0$.

phase close to the isotopic substitution. On physical grounds, we can expect liquid bubbles of host atoms to appear close to the guest isotope. Unfortunately, since the present analysis is only related to the stability condition of the solid phase, we are not able to estimate the size of the liquid bubble, and more sophisticated approaches are needed. It is interesting to note that, for quantum solids, the critical temperature T_c^{Qimp} for the local stability of the solid phase close to the quantum isotope impurity is reduced with respect to the bulk T_c. This is shown in the bottom panel of Fig. 3 where the ratio between the local T_c close to the impurity and the bulk T_c is plotted as a function of the quantum degree of the system, parametrized by τ_H. In the quantum regime, where T_c^{Qimp}

$\lesssim \hbar\tilde{\omega}_0/4$, the local melting temperature T_c^{Qimp} can be significantly lower than the one in the bulk T_c, and, for $1.39 < \tau_{\mathrm{H}e} < 2$, we expect a quantum isotopic impurity to induce local melting down to $T=0$, although the bulk phase is still stable.

VI. DISCUSSION AND CONCLUSIONS

In this paper, we have investigated the stability of quantum solids with respect to surface melting and to isotopic quantum substitutions. Both these phenomena can be essentially related to the amount of lattice fluctuations, and they can be driven thus by thermal fluctuations as well as by the zero point quantum motion. We have shown that the effects of isotopic impurities and surface melting are strongly enhanced in quantum solids. In particular, we show that when quantum fluctuations are dominant in quantum solids, the solid phase can be rapidly destroyed on the surface and close to quantum impurities at temperatures much smaller than for the bulk melting.

Helium solids are the natural candidates where the quantum instabilities of surface or interface can occur. The actual relevance of these quantum melting effects is of course ruled by the magnitude of the quantum lattice fluctuations which are parametrized in our model by the quantity τ_{Q}. An accurate calculation of the quantum lattice fluctuations as a function of the temperature in ^{4}He and ^{3}He solids has been provided recently, by using of quantum Monte Carlo (QMC) techniques, by Draeger and Ceperley in Ref. 25, in excellent agreement with the experimental data.[24] Quite interestingly, they find that the mean square lattice displacement $\langle u^2\rangle_T$ does not follow at low temperature an harmonic behavior $\langle u^2\rangle_T \simeq \langle u^2\rangle_{T=0} + \alpha T^2$, but rather a more shallow one, $\langle u^2\rangle_T \simeq \langle u^2\rangle_{T=0} + \beta T^3$.

Reference 25 represents a suitable source to estimate an effective value of τ_{Q}, representative of solid helium. To this aim, we fit the temperature dependence of the QMC data of Ref. 25 with our quantum SCHA model described by Eq. (12), where only two independent fitting parameters appear, namely, λ and k_0 (remind that $\tau_{\mathrm{cl}}=\lambda k_B T/k_0$, $\tau_{\mathrm{Q}}=\lambda\hbar/2\sqrt{k_0 M}$). The fit of our quantum SCHA [Eq. (12)] compared with the QMC data is shown in Fig. 4 for three representative cases, where the number of numerical data is larger than the number of independent fitting parameters to guarantee the significance of the fitting procedure. Also shown is the fit with a purely harmonic model obtained by setting $\lambda=0$. The extracted values of λ and k_0, as well as of the corresponding τ_{Q} and of the anharmonic renormalized phonon frequency $\tilde{\omega}_0$ at $T=0$ are reported in Table I, where we also report the critical temperature T_c for the solid phase bulk instability evaluated within the SCHA and the experimental melting temperature T_m^{exp}.[22,28]

It is worth commenting on the temperature behavior of the QMC data compared with the harmonic ($\lambda=0$) and anharmonic SCHA fits. An important point to be underlined here is that QMC results show a *large* mean square lattice displacement at zero temperature together with a rapidly turn up of $\langle u^2\rangle$ close to the solid bulk instability. As we have discussed in Sec. III, this is a characteristic trend of highly quantum solids. On the other hand, this behavior is poorly reproduced by a purely harmonic model where the amount of the lattice fluctuations at $T=0$ is inversely proportional to the temperature dependence. This is even more true if a Debye model would be employed since the temperature dependence

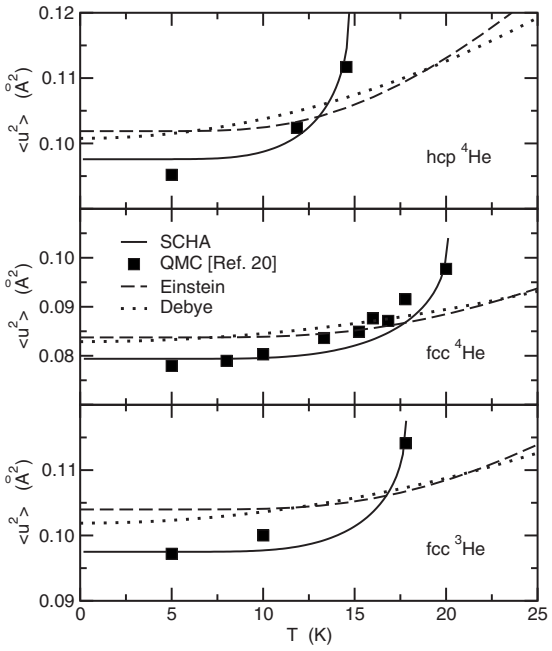

FIG. 4. Lattice fluctuations $\langle u^2\rangle$ evaluated within the SCHA (solid lines) as a function of temperature for different helium solid conditions compared with quantum Monte Carlo data of Ref. 25. Values of k_0 and λ in SCHA obtained by fitting QMC data are reported in Table I. Also shown is the purely harmonic fitting of the QMC data with a Einstein and a Debye model.

TABLE I. Values of k_0 and λ in SCHA obtained by fitting the QMC data of Ref. 25 for three representative helium solids, namely, hcp ^{4}He at molar volume $V_0=12.12$ cm^3/mole, fcc ^{4}He at molar volume $V_0=10.98$ cm^3/mole, and fcc ^{3}He at molar volume $V_0=11.54$ cm^3/mole. Also reported are the corresponding values of τ_{Q}, the renormalized phonon frequency $\tilde{\omega}_0$, and the predicted critical temperature T_c of the solid phase bulk instability compared with the experimental melting temperature T_m^{exp} (Ref. 22 and 28).

	hcp ^{4}He	fcc ^{4}He	fcc ^{3}He
V_0 (cm^3/mole)	12.12	10.98	11.54
k_0 (meV/Å^2)	110 ± 10	140 ± 10	150 ± 10
λ (Å^{-2})	14 ± 1	15.2 ± 0.8	14.7 ± 0.7
τ_{Q}	0.69 ± 0.08	0.66 ± 0.06	0.70 ± 0.06
$\tilde{\omega}_0$ (meV)	4.6 ± 0.1	5.4 ± 0.4	6.1 ± 0.5
T_c (K)	14 ± 4	20 ± 4	18 ± 4
T_m^{exp} (K)	~15	~21	~22

of a Debye model is even shallower than in the Einstein case.

The strong quantum degree of solid helium, qualitatively predicted by these arguments, is confirmed by the numerical analysis of the SCHA fit which predicts a quantum parameter τ_Q in the range $\tau_Q \simeq 0.66-0.7$ for the three samples considered. Here, the robustness of our fits is confirmed by the nice agreement between the critical temperature for the bulk instability of the solid phase estimated by the SCHA and the experimental melting temperature.

These results have important consequences with respect to the surface and/or grain-boundary melting instability and local melting induced by quantum isotopic impurities. The value of $\tau_Q \simeq 0.69$, for the low pressure and/or high molar volume $V_0 = 12.12$ cm^3/mole, is safely larger than the value $\tau_Q^{SM} \simeq 0.664$ where surface melting occurs at zero temperature and/or the same order and slightly larger even than $\tau_Q^{SM} \simeq 0.681$ where isotopic impurity induced melting also occurs at zero temperature. Although these estimates are only indicative of the quantum degree of helium solid, they clearly point out that quantum anharmonic effects are large enough in solid helium, for these or larger molar volumes, to enforce surface melting and local melting close to quantum impurities *down to zero temperature*. Quantum Monte Carlo simulations have actually confirmed premelting at surface between helium solid and Vycor walls[29] and internal interfaces of a pure helium system,[30] although not all possible interfaces undergo a solid and/or liquid transition.

These results shed an interesting light also on the recent report of the nonclassical rotational inertia (NCRI) observed in ^{4}He.[31,32] While it was initially claimed to be an evidence of a supersolid (SS) phase, subsequent experiments showed a strong dependence of the NCRI on the annealing process,[33] on the presence of grain boundaries,[34] on the amount of ^{3}He concentration,[32,35,36] as well as on the freezing procedure.[35,36] These observations give rise to an alternative hypothesis to the SS phase, namely, that a liquid phase is confined at the grain boundaries and that mass flow is related to superfluidity of the liquid component.[37] Our results confirm this scenario and shed interesting perspectives about the role of disorder and/or grain boundaries in solid helium. In particular, we provide a natural explanation for the existence of a liquid (and thus probably superfluid) phase at the grain boundaries and we *predict* a local liquid phase also around ^{3}He impurities. Local melting close to isotopic ^{3}He impurities should be, thus, explicitly considered.

ACKNOWLEDGMENTS

This work was supported by the Italian Research Programs MIUR PRIN 2005 and PRIN 2007. G.R. acknowledges useful discussions with M. Holzmann and D. M. Ceperley.

[1] J. G. Dash, Rev. Mod. Phys. **71**, 1737 (1999).
[2] H. Lowen, Phys. Rep. **237**, 249 (1994).
[3] M. Forsblom and G. Grimvall, Nat. Mater. **4**, 388 (2005).
[4] F. Lindemann, Z. Physiother. **11**, 609 (1910).
[5] J. J. Gilvarry, Phys. Rev. **102**, 308 (1956).
[6] M. Ross, Phys. Rev. **184**, 233 (1969).
[7] G. Grimvall and S. Sjödin, Phys. Scr. **10**, 340 (1974).
[8] Z. H. Jin, P. Gumbsch, K. Lu, and E. Ma, Phys. Rev. Lett. **87**, 055703 (2001).
[9] A. M. Alsayed, M. F. Islam, J. Zhang, P. J. Collings, and A. G. Yodh, Science **309**, 1207 (2005).
[10] L. Pietronero and E. Tosatti, Solid State Commun. **32**, 255 (1979).
[11] A. Trayanov and E. Tosatti, Phys. Rev. B **38**, 6961 (1988).
[12] For a review, see, U. Tartaglino, T. Zykova-Timan, F. Ercolessi, and E. Tosatti, Phys. Rep. **411**, 291 (2005).
[13] P. Brüesch, *Phonons: Theory and Experiments III*, Springer Series in Solid State Sciences (Springer, Berlin, 1987), Vol. 66.
[14] E. Polturak and N. Gov, Contemp. Phys. **44**, 145 (2003).
[15] G. Senatore and G. Pastore, Phys. Rev. Lett. **64**, 303 (1990).
[16] S. Moroni and G. Senatore, Phys. Rev. B **44**, 9864 (1991).
[17] C. N. Likos, S. Moroni, and G. Senatore, Phys. Rev. B **55**, 8867 (1997).
[18] A. R. Denton, P. Nielaba, K. J. Runge, and N. W. Ashcroft, Phys. Rev. Lett. **64**, 1529 (1990); J. Phys.: Condens. Matter **3**, 593 (1991).
[19] J. D. McCoy, S. W. Rick, and A. D. J. Haymet, J. Chem. Phys. **90**, 4622 (1989); **92**, 3034 (1990); S. W. Rick, J. D. McCoy, and A. D. J. Haymet, *ibid.* **92**, 3040 (1990).
[20] D. M. Ceperley and G. Jacucci, Phys. Rev. Lett. **58**, 1648 (1987).
[21] D. M. Ceperley and B. Bernu, Phys. Rev. Lett. **93**, 155303 (2004).
[22] J. Wilks, *The Properties of Liquid and Solid Helium* (Claredon, Oxford, 1967).
[23] H. R. Glyde, in *Encyclopedia of Physics*, edited by R. G. Lerner and G. L. Trigg, Vol. 1 (Wiley, Berlin, 2005).
[24] D. A. Arms, R. S. Shah, and R. O. Simmons, Phys. Rev. B **67**, 094303 (2003).
[25] E. W. Draeger and D. M. Ceperley, Phys. Rev. B **61**, 12094 (2000).
[26] P. Loubeyre and J. P. Hansen, Phys. Lett. **80A**, 181 (1980).
[27] M. Boninsegni, C. Pierleoni, and D. M. Ceperley, Phys. Rev. Lett. **72**, 1854 (1994).
[28] E. R. Dobbs, *Helium Three* (Oxford University, Oxford, 2000).
[29] S. A. Khairallah and D. M. Ceperley, Phys. Rev. Lett. **95**, 185301 (2005).
[30] L. Pollet, M. Boninsegni, A. B. Kuklov, N. V. Prokof'ev, B. V. Svistunov, and M. Troyer, Phys. Rev. Lett. **98**, 135301 (2007).
[31] E. Kim and M. H. W. Chan, Nature (London) **427**, 225 (2004).
[32] E. Kim and M. H. W. Chan, Science **305**, 1941 (2004).
[33] Ann Sophie, C. Rittner, and J. D. Reppy, Phys. Rev. Lett. **98**, 175302 (2007).
[34] S. Sasaki, R. Ishiguro, F. Caupin, H. J. Maris, and S. Balibar, Science **313**, 1098 (2006).
[35] A. C. Clark, J. T. West, and M. H. W. Chan, Phys. Rev. Lett. **99**, 135302 (2007).
[36] E. Kim, J. S. Xia, J. T. West, X. Lin, A. C. Clark, and M. H. W. Chan, arXiv:0710.3370 (unpublished).
[37] E. Burovski, E. Kozik, A. Kuklov, N. Prokof'ev, and B. Svistunov, Phys. Rev. Lett. **94**, 165301 (2005).